

Theoretical Seismic Waveform Calculation with an Accuracy of 1.6 Seconds by the Spectral Element Method

Project Representative

Seiji Tsuboi Center for Earth Information Science and Technology, Japan Agency for Marine-Earth Science and Technology

Authors

Seiji Tsuboi *¹, Rhett Butler *²

*¹Center for Earth Information Science and Technology, Japan Agency for Marine-Earth Science and Technology,

*²University of Hawaii

Keywords : spectral element method, theoretical seismograms, antipodal observation, inner core outer core boundary, low velocity zone

1. Introduction

The fluid nature of Earth's outer core was determined by Jeffreys (1926)[1], followed in 1936 with Lehmann's (1936)[2] discovery of the solid inner core. Birch (1952)[3] summarized available data and concluded the core is an iron alloy with a small component of lighter elements. This inner-outer core boundary (IOCB) separates the freezing, growing inner core from the convecting outer core which drives the dynamo generating Earth's magnetic field (Verhoogen, (1961); Braginsky, (1963); Gubbins, (1977); Loper, (1978); Butler and Anderson, (1978); Stevenson, (1987); Cormier et al. (2011); Monnereau et al. (2010); Alboussière et al., (2010)). [4-12].

As in our 2022 ES4 report, and in a paper submitted to Physics of the Earth and Planetary Interior, we approach this analysis of the basal outer core boundary (BOC) with antipodal waveform data in the distance range 179.0°–180° to test the hypothesis whether propagation at the BOC is commensurate with diffraction and/or refraction. The propagation paths observed envelop about two-thirds of the IOCB surface. The adequacy of global core and 3-D mantle models (e.g., PREM, Dziewonski and Anderson, 1981; Kustowski et al., 2008) [13-14] in fitting the antipodal observations is found to be deficient.

2. Modeling

In this report, we have extended the antipodal analysis to include significant attenuation at the BOC (Fig. 1). This approach was undertaken to clarify “ringing” following the arrival of C_{diff} in the synthetic waveform, postulated to be due refraction in a low velocity zone (LVZ) at the BOC. For PREM the attenuation at the BOC is characterized by a bulk $Q_k = 57288$. As the antipodal propagation traverses about 850 km at the BOC, a simple calculation shows that in reducing Q_k from 57822 to 120, the amplitude and duration of C_{LVZ} ringing should be reduced. Two, thin LVZ models are tested—a 20 km thick layer, and a negative gradient from 50 km thick to the IOCB—with a velocity of 10.0 km/s. Synthetic modeling of the thin, low velocity structures requires higher resolution (1.6 sec) parametrization to achieve necessary detail.

We synthesized in Fig. 2 the antipodal data at the Qiongzong

(QIZ) station in China due to the April 17, 2009 earthquake in northern Chile (Mw6.1). Comparing the two Q models in blue (120) and black (57288), they are nearly identical. This suggests that the simple approximation of the effect of increased attenuation at the BOC is more complex than can be ascribed to simple layers. Possible considerations include lower values of Q in the BOC, a transition zone between the high Q outer core and low Q BOC, or a frequency dependent Q. Each possibility must also be reconciled with possible models of attenuation in an iron-nickel alloy, or as alloyed with a lighter, faster element(s). Further synthesis and analysis using the Earth Simulator-4 may answer these questions.

3. Theoretical seismograms

We have performed global seismic wave propagation calculations using the spectral element method, which is a type of finite element method, for a realistic earth model—(Komatitsch and Vilotte, 1998; Komatitsch et al., 2002; Tsuboi et al., 2003; Komatitsch et al., 2005)[15-18] as previously applied (Butler and Tsuboi, 2010; Tsuboi and Butler, 2020; Butler and Tsuboi, 2020, Butler and Tsuboi, 2021)[19-22]. In 2016, we used the K computer's 82,134 nodes (99% of all nodes) by dividing

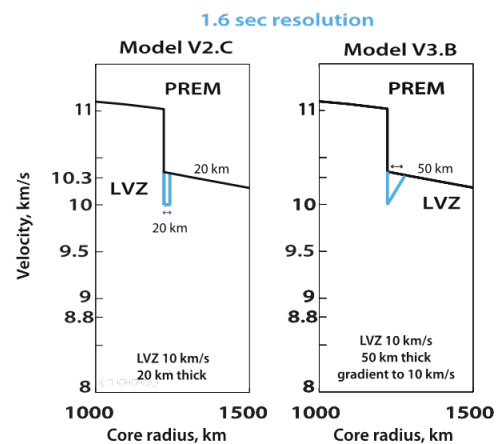


Figure 1. The models shown here are based upon PREM + 3D

mantle, with modifications (light blue) at the IOCB. Models were initially calculated at 3.5 sec resolution. For a velocity of 10 km/s this wavelength is about 50 km, which is larger than the modeled structure. To achieve the requisite resolution, the 3DSEM were synthesized at 1.6 s resolution. The models tested considered discontinuous velocity changes at the base of the outer core in layers 20 km thick with $V_p = 10$ km/s, as well as a negative gradient to $V_p = 10$ km/s at the bottom 50 km of the IOCB. In modeling bulk attenuation at the BOC, $Q_k = 120$ in the light blue layers.

the earth model into 665.2 billion grid points to perform theoretical seismic waveform recording calculations with an accuracy of about 1.2 seconds. (Tsuboi et al., 2016)[23]. This time, we report that the same scale of calculation was performed by the Earth Simulator (ES4) system

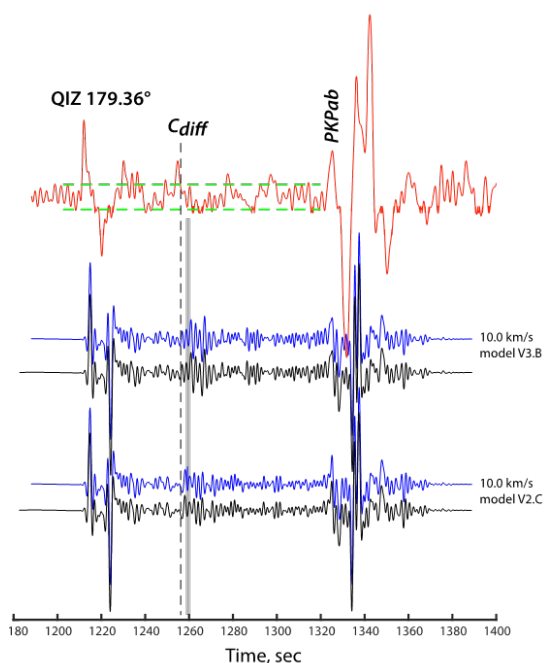


Figure 2. The model series plots the 3-D synthetics fits to QIZ 2009 for models in Fig. 1. The antipodal data are in red. The synthesized models are computed at a 1.6 s resolution. At the BOC Q_k is set to 120 and 57822 in the synthetics shown in blue and black, respectively. The waveforms are aligned on PKPab, which unlike PKIKP does not interact with the IOCB. The dashed line is the PREM theoretical Cdiff arrival time, whereas the gray line is aligned on the timing of slant stacked QIZ Cdiff data. The blue and black traces are nearly identical, showing that smaller values of Q (higher attenuation) would be needed to reduce the duration of ringing after Cdiff.

In the calculation of the spectral element method, the division of the earth model divides the entire earth into six quadrangular pyramids, and each quadrangular pyramid is divided into finer quadrangular pyramids and assigned to individual CPUs of the

supercomputer to perform the calculation. In this calculation, the theoretical seismic waveform propagating globally with an accuracy of 1.6 seconds was calculated by dividing it into 244.7 billion grid points. The parameters NEX and NPROC indicating the division of the spectral element method in this case are 2656 and 83, respectively, and the total number of cores used in the calculation is 41,334 and the ES4 vector engine (VE) is 5168. The grid point spacing in this mesh is 0.94 km on average. For this scale of calculation, it took about 30 minutes CPU time to calculate the mesh and 4 hours 40 minutes CPU time to calculate the theoretical seismic waveform for 23 minutes. The size of the mesh is about 41 Tbyte. The calculation used NEC's MPI as a flat MPI, and the effective performance according to the MPI Program Information was 1.13 PFLOPS, and the vectorization rate was 99%. This effective performance is about 8.8% of the theoretical peak performance of 5168VE.

Acknowledgment

Data were obtained from GEOSCOPE and the IRIS Data Management System. We used the computer program (SPECFEM3D) for Spectral-Element Method. Centroid moment tensor solutions (GCMT) are used for synthetic models. We thank GEOSCOPE, USGS and NSF, NCDSN China, and the Spanish Digital Seismic Network for the operation and maintenance of the seismic stations used in this study.

References

- [1]. Jeffreys, H., 1926. The rigidity of the Earth's central core. *Mon. Not. R. Astron. Soc. Geophys.* 1, 371–383.
- [2]. Lehmann, I., 1936. P': Bureau Central Seismologique International Strasbourg, 14. *Publications du Bureau Central Scientifiques*, pp. 87–115.
- [3]. Birch, F. (1952). Elasticity and constitution of the Earth's interior. *J. Geophys. Res.* 57, 227–286 (1952).
- [4]. Verhoogen, J., 1961. Heat balance of the Earth's core. *Geophys. J. R. Astron. Soc.* 4, 276–291.
- [5]. Braginsky, S., 1963. Structure of the F layer and reasons for convection in the Earth's core. *Dokl. Akad. Nauk. SSSR Engl. Trans.* 149, 1311–1314.
- [6]. Gubbins, D., 1977. Energetics of the Earth's core, *J. Geophys.*, 43, 453–464.
- [7]. Loper, D.E., 1978. The gravitationally powered dynamo, *Geophys. J. R. astr.Soc.*, 54, 389–404.
- [8]. Butler, R. and Anderson, D.L., 1978. Equation of state fits to the lower mantle and outer core. *Physics of the Earth and Planetary Interiors*, 17(2), pp.147–162.
- [9]. Stevenson, D.J., 1987. Limits on lateral density and velocity variations in the Earth's outer core. *Geophysical Journal International*, 88(1), pp.311–319.
- [10]. Cormier, V.F., Attanayake, J. and He, K., 2011. Inner core freezing and melting: Constraints from seismic body waves.

- Physics of the Earth and Planetary Interiors, 188(3-4), pp.163-172.
- [11]. Monnereau, M., Calvet, M., Margerin, L., Souriau, A., 2010. Lopsided growth of Earth's inner core. *Science* 1014-1017.
- [12]. Alboussière, T., Deguen, R., Melzani, M., 2010. Melting induced stratification above Earth's inner core due to convective translation. *Nature* 466, 744-747.
- [13]. Dziewonski, A.M., Anderson, D.L., 1981. Preliminary reference Earth model. *Physics of the Earth and Planetary*, 25, 297-356.
- [14]. Kustowski, B., Ekström, G., Dziewonski, A.M., 2008. Anisotropic shear-wave velocity structure of the Earth's mantle: a global model. *J. Geophys. Res. Solid Earth* 113 (B6).
- [15]. Komatitsch, D., Vilotte, J.P., 1998. The spectral-element method: an efficient tool to simulate the seismic response of 2D and 3D geological structures. *Bull. Seismol. Soc. Am.* 88, 368-392.
- [16]. Komatitsch, D., Ritsema, J., Tromp, J., 2002. The spectral-element method, Beowulf computing, and global seismology. *Science* 298, 1737-1742.
- [17]. Tsuboi, S., Komatitsch, D., Ji, C., Tromp, J., 2003. Broadband modeling of the 2002 Denali fault earthquake on the earth simulator. *Phys. Earth Planet. Inter.* 139, 305-312.
- [18]. Komatitsch, D., Tsuboi, S., Tromp, J., 2005. The spectral-element in seismology. In: Levander, A., Nolet, G. (Eds.), *Seismic Earth: Array Analysis of Broadband Seismograms*, AGU Geophysical Monograph 157. AGU, pp. 205-227.
- [19]. Butler, R. and Tsuboi, S., 2010. Antipodal seismic observations of temporal and global variation at Earth's inner - outer core boundary. *Geophysical Research Letters*, 37(11).
- [20]. Tsuboi, S. and R. Butler, 2020. Inner core differential rotation rate inferred from antipodal seismic observations. *Physics of Earth and Planetary Interiors*, 301, April 2020, 106451, doi.org/10.1016/j.pepi.2020.106451+Auxiliary Material
- [21]. Butler, R. and S. Tsuboi, 2020. Antipodal Observations of Global Differential Times of Diffracted P and PKPAB within the D'' Layer above Earth's Core-Mantle Boundary, *Geophysical Journal International*, 220, , doi.org/10.1093/gji/ggaa157
- [22]. Butler, R. and Tsuboi, S., 2021. Antipodal seismic reflections upon shear wave velocity structures within Earth's inner core. *Physics of the Earth and Planetary Interiors*, 321, p.106802.
- [23]. Tsuboi, S., K. Ando, T. Miyoshi, D. Peter, D. Komatitsch, J. Tromp, 2016. A 1.8 trillion 627 degrees-of-freedom, 1.24 petaflops global seismic wave simulation on the K computer, *International Journal of High Performance*